

Palladium Terminal Imido Complexes with Nitrene Character

Annette Grünwald,^{a,b} Bhupendra Goswami,^a Kevin Breitwieser,^a Bernd Morgenstern,^a Martí Gimferrer,^c Frank W. Heinemann,^b Dajana M. Momper,^{a,d} Christopher W. M. Kay,^{d,e} Dominik Munz^{*a,b}

^a Saarland University, Coordination Chemistry, Campus C4.1, D-66123 Saarbrücken, Germany;

^b Friedrich-Alexander-Universität Erlangen-Nürnberg, Inorganic and General Chemistry, Egerlandstr. 1, D-91058 Erlangen, Germany;

^c Institut de Química Computacional i Catàlisi and Departament de Química, Universitat de Girona, Campus Montilivi, 17003, Girona, Catalonia, Spain;

^d Saarland University, Physical Chemistry, Campus B2.2, D-66123 Saarbrücken, Germany.

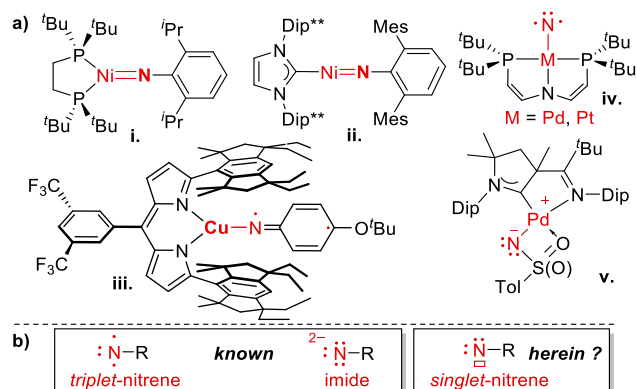
^e London Centre for Nanotechnology, University College London, 17-19 Gordon Street, London WC1H 0AH, UK.

Nitrene, Imido, Late Transition Metals, Multiple Bonds, Electronic Structure, CH activation, CF activation

ABSTRACT: Whereas triplet-nitrene complexes of the late transition metals are isolable and key intermediates in catalysis, singlet nitrene ligands remain elusive. Herein, we communicate three such palladium terminal imido complexes. UV-Vis/NIR electronic spectroscopy with broad bands up to 1400 nm as well as high-level computations DFT, STEOM-CCSD, CAS-SCF/NEVPT2, EOS analysis) and reactivity studies suggest significant palladium(0) singlet-nitrene character. Although the aliphatic nitrene complexes proved too reactive for isolation in analytically pure form due to elimination of isobutylene, the aryl congener could be characterized by SC-XRD, elemental analysis, IR, HRMS and NMR spectroscopy. The complexes' distinguished ambiphilicity allows them to activate hexafluorobenzene, triphenylphosphine and pinacol borane, catalytically dehydrogenate cyclohexene, and aminate ethylene *via* nitrene transfer at (or below) room temperature.

Imido complexes of early transition metals are textbook examples for multiple bonding. For decades, it was believed that the late transition metal congeners are too reactive to be isolated due to their populated metal–ligand antibonding molecular orbitals.^{1,2} Notwithstanding, Mindiola, Waterman and Hillhouse studied a formally d^8 -configured nickel terminal imido complex (Chart 1a, **i**).³⁻⁴ Further nickel complexes including **ii**, followed,⁵⁻¹¹ and a crystalline copper nitrene pertinent to CH amination was also described (**iii**).¹² The heavier $4d$ and $5d$ elements are less explored.¹³⁻¹⁵ Yet, Schneider and colleagues investigated the transient triplet nitrenes **iv**.¹⁶⁻¹⁷

Chart 1. Isolated imido complexes with a formal d^8 (or higher) electron configuration (top) and leading resonance structures of imido complexes (bottom).



Commonly, all these complexes present low-lying triplet excited states or even, as is the case for **ii**–**iv**, triplet ground states.¹⁸ Indeed, triplet-nitrene character,¹⁹ *viz.* a triplet nitrogen ligand with a valence-electron sextet (Chart 1b, bottom left), is thought to be crucial for nitrene transfer catalysis by transient coinage metal imido complexes.²⁰⁻²² In search for singlet-nitrene complexes (Chart 1b, bottom right),²³⁻²⁵ we contributed **v**. [L_2Pd (NSO₂Tol)].²⁶⁻²⁷ This complex profits from the strong ligand field exerted by the ancillary cyclic (alkyl)(amino) carbene (CAAC) and hyperconjugation with the sulfonyl substituent. Consequently, it shows a zwitterionic, closed-shell electronic structure (Chart 1b, bottom middle) with a nucleophilic imide-type ligand.²⁸⁻³⁰ Herein, we communicate that less-stabilizing aliphatic and aromatic substituents afford tri-coordinate **2**, **3** and **4**, which may be understood as zerovalent singlet nitrene complexes. Distinct to triplet nitrenes and radical imidyl ligands, they are strongly ambiphilic and swiftly activate C–F and C–H bonds at or below room temperature.

Thawing benzene solutions of a mixture of red **1**³¹ and 2,6-diisopropylphenyl- (Dip-), *tert*-butyl- (^tBu-) or adamantyl (Ad-) azide (Fig. 1, left) led to an instantaneous color change to intense green. Immediately recorded ¹H NMR spectra indicated the clean formation of **2**, whereas in case of **3** and **4** minor (≈ 10 – 20%) amounts of byproducts were already discernible. Benzene solutions of **2** converted with $t_{1/2} < 2$ h (Figs. S4, S5) to hitherto unidentified products (for **3**, see Scheme 1e). The presence of an excess (20 equivalents) of organic azide enhanced the complexes' persistence (**3**, $t_{1/2} \approx$

4 min; **4**, $t_{1/2} \approx 25$ min; Figs. S8, S9, S12, S13). Conversion occurred faster (pyridine, toluene [**3**, $t_{1/2} \approx 3$ min]) or at comparable rates (hexane, diethyl- or *tert*-butyl methyl ether) in other solvents. Complex **2** could be isolated by lyophilizing and recrystallizing from hexanes at -40 °C. Single-crystals suitable for X-ray diffractometry were obtained through cooling (-40 °C) a saturated hexane solution spiked with tetrahydrofuran. The solid state structure of **2** (Fig. 1, right) exhibited a disorder of the CAAC ligand. This disorder can be described by an approximated mirror plane perpendicular to the plane of the phenyl ring C37 – C38 and roughly running along the N3 – C37 – C40 line (Fig. S62). The molecular structure of tris-coordinate **2** exhibits a bent ($160.3(3)^\circ$) Pd-N-C linkage. The Pd-N^{Dip} bond length of $1.872(3)$ Å is short in respect to anilido complexes (>2.0 Å) and imide **v**. ($2.042(2)$ Å) and in the range of computed palladium nitrenes ($1.8 - 2.0$ Å),²³ as well as pallada-nitrene **iv**. ($1.92(2)$ Å).¹⁷

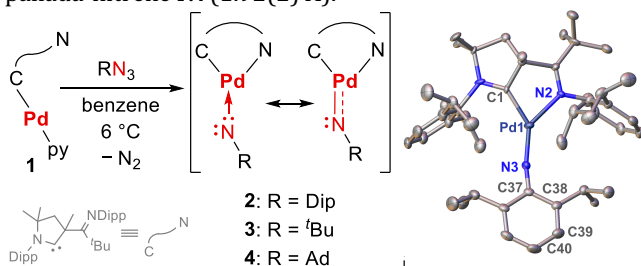


Figure 1. Synthesis (left) and solid-state structure of **2** (right). Alternative orientation of **2**, cocrystallized THF molecules, as well as H-atoms are omitted for clarity. Selected bond lengths [Å] and angles [°]: Pd1–N3, $1.872(3)$; Pd1–C1, $1.947(4)$; Pd1–N2, $2.118(5)$; N3–C37, $1.340(4)$; C37–C38, $1.432(4)$; C38–C39, $1.394(5)$; C39–C40, $1.381(6)$; C37–N3–Pd1 $160.3(3)$; N3–Pd1–C1, $145.7(2)$; N3–Pd1–N2, $137.4(2)$.

Moderate¹³ mesomeric stabilization by the aromatic substituent is observed [N3–C37, $1.340(4)$ Å; C37–C38, $1.432(4)$; C38–C39, $1.394(5)$ Å]. Crystallization attempts for **3** and **4** from neat *tert*-butyl azide and aliphatic solvents afforded only decomposition products such as the deprotonation of the CAAC's backbone and formation of a palladium(II) amide (Fig. S64), thus suggesting high basicity of **3**.

Consequently, we sought to trap transient **3** and **4** with a weak electrophile. Hexafluorobenzene was chosen, since synthesizing palladium(II) fluoro complexes is a challenge in sight of excessive hard/soft mismatch. However, **3** and **4** reacted instantaneously even at -40 °C, and the ¹⁹F spectroscopic analysis (Figs. S15, S19) indicated that (pentafluorophenylamido)(fluoro) palladium(II) complexes formed (Fig. 2, left). The molecular structure of single-crystals of **5** corroborated the 1,2-addition of one C–F bond (Fig 2, right). Complex **2** was less reactive and, thus, neat C_6F_6 was required to bring it to reaction at room temperature (Fig. S20).

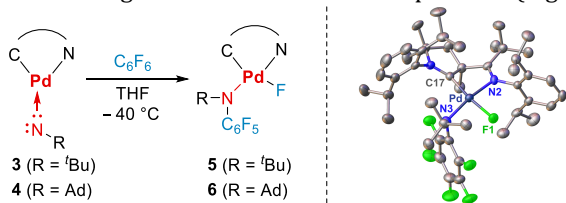
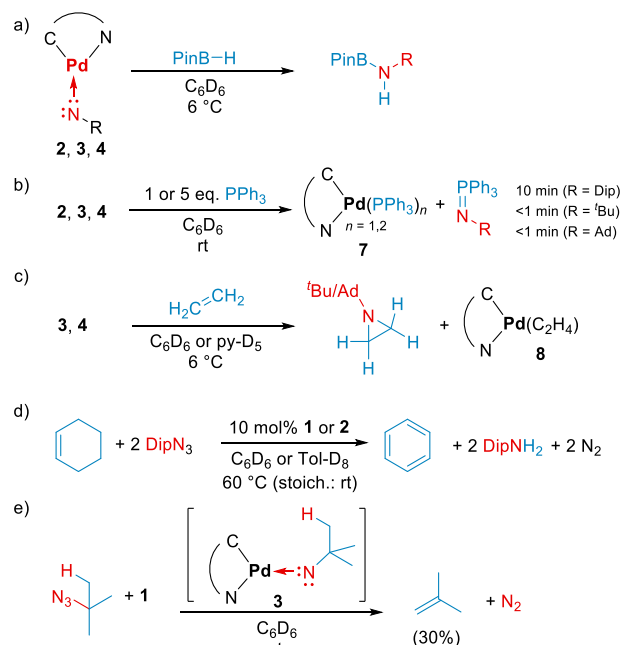


Figure 2. C_6F_6 activation (left) and structure of **5** in the solid state (right). Hydrogen atoms are omitted for clarity. Selected bond lengths [Å] and angles [°]: Pd–N3, $2.081(4)$; Pd–C17, $1.961(4)$; Pd–N1, $2.071(4)$; Pd–F1, $1.994(3)$; C17–Pd–N3, $103.65(2)$.

Similarly, instantaneous B–H insertion was observed in case of pinacol borane (Scheme 1, a). We also probed the reaction with a nucleophile, namely triphenylphosphine (Scheme 1, b). The respective iminophosphoranes formed in case of **3** and **4** instantaneously, whereas the reaction with **2** required a couple of minutes to reach completion. Elucidating the reactivity with olefins, **2**, **3** and **4** were treated with ethylene (Scheme 1, c) and cyclohexene (Scheme 1, d). In the reaction with ethylene, immediate nitrene transfer from **3** and **4** gave the respective aziridines, whereas the four-membered palladacycle formed with **2** (Fig. S39). Interestingly, the reaction of **2** with cyclohexene gave benzene. The stoichiometric reaction proceeds slowly at room temperature (17% conversion after 4 days), yet quantitative yield was obtained after heating to 60 °C under catalytic (10 mol% **1** or **2**) conditions. To probe for long-lived radical intermediates,³² EPR spectroscopy was employed, yet no such signatures were detected. Peculiar reactivity was observed for **3**, which gave isobutylene in 30% spectroscopic yield (Scheme 1, e).³³ This transformation represents overall a rare³⁴ formal β -elimination of HN_3 , although it is mechanistically distinct due to the formation of N_2 .

Scheme 1. Reactivity of **2**, **3** and **4** with PPh_3 , ethylene, cyclohexene, and HBPIn as well as formation of isobutylene from **3**. All reactions proceed, if not otherwise indicated, with quantitative spectroscopic yield.



Targeting the electronic structure, infrared spectra of **2** were recorded. Yet, no feature could be unambiguously assigned to the Pd=N stretch (Fig. S3). UV-Vis/NIR spectroscopic measurements proved more productive (Fig. 3). The electronic spectra of complexes **2**, **3** and **4** are similar with intense ($\epsilon \approx 4-6 \times 10^4 M^{-1} cm^{-1}$) and for palladium unusual

features in the green (**2**, $\lambda_{\text{max}} = 685$ nm; **3**, $\lambda_{\text{max}} = 622$ nm; **4**, $\lambda_{\text{max}} = 638$ nm) as well as red ($\lambda \approx 480$ nm) range of the spectrum, and weaker ($\epsilon = < 10^4$ M⁻¹ cm⁻¹) bands in the NIR (**2**, $\lambda \approx 1200$ nm; **3, 4**, $\lambda \approx 900$ nm).

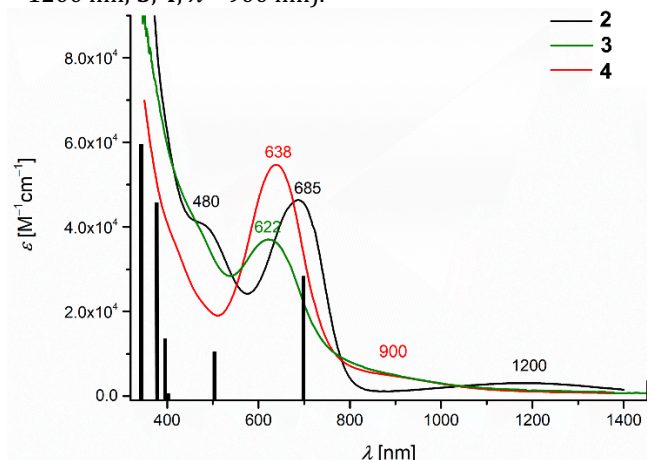


Figure 3. Electronic absorption spectra of **2**, **3** and **4** in methyl *tert*-butyl ether and STEOM-CCSD calculated transitions (black bars) for **2**.

Importantly, these bands are different to the ones of yellow sulfonimido complex **v**, yet similar in shape and red-shifted in comparison with bands assigned to transient copper⁻³⁵⁻³⁷ and free nitrenes.³⁸ Scalar-relativistic (ZORA) STEOM-CCSD calculations reproduce the bands excellent (Fig. 3; Figs. S70–S71).³⁹ To understand these transitions and the underlying electronic structures, CASSCF/NEVPT2 calculations were performed for **2**, **3** and **4**. Their vertical singlet/triplet energy gaps are predicted to be moderate with $\Delta E^{S/t} = 0.93$ eV for aromatic **2** and 1.16 and 1.14 eV for aliphatic **3** and **4**.

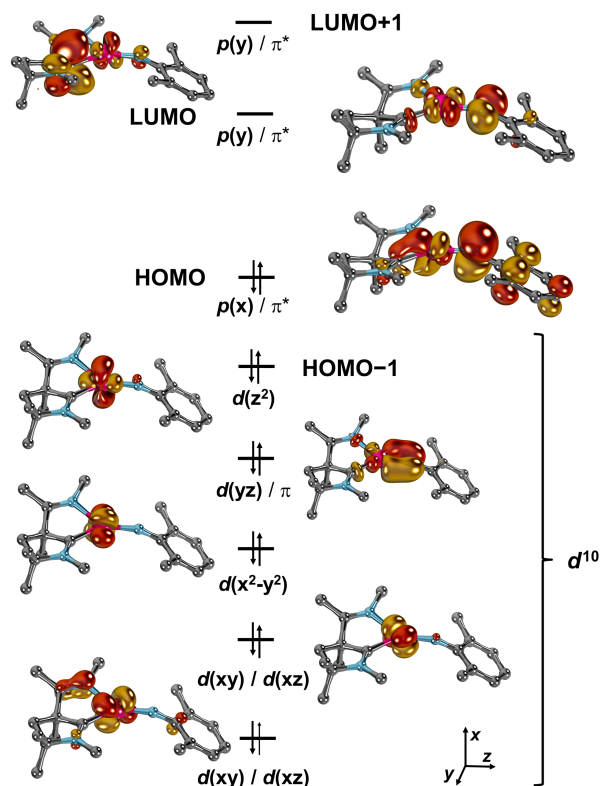


Figure 4. Natural orbitals in truncated model system of **2** according to sa-CASSCF(16,11) calculations (lead configuration: $c = 0.49$),⁴⁰ orbital energies are chosen for clarity. See Figs. S109–S112 for further details and Dip-centered π - and π^* orbitals.

As illustrated for **2** (Fig. 4), four non-bonding $4d$ -orbitals [$d(xy)$, $d(xz)$, $d(x^2-y^2)$, $d(z^2)$] are doubly occupied. As is allowed in idealized C_s symmetry, the $d(xy)$ and $d(yz)$ - as well as the $d(x^2-y^2)$, $d(z^2)$ and $5s$ orbitals mix. This explains the coordination of the imino-ligand upon nitrene-complex formation. The bonding π -interaction associated with the $d(yz)$ orbital is covalent according to visual inspection. However, applying Löwdin's population analysis suggests that it is rather metal centered (Pd : N = 0.7 : 0.3). The HOMO is clearly N -donor centered (Pd : N = 0.2 : 0.8) with moderate admixture of the CAAC- and Dip π -systems. Overall, this assignment gives rise to a zero-valent metal according to IUPACs "winner takes it all" definition.⁴¹ Consistent electronic structures were obtained for **3** and **4** (Fig. S125–S152). Chemical bonding tools were applied at the DFT (PBE, PBE0) level of theory, including bond orders (Mayer, Wiberg) using diverse Hilbert- (Mulliken, Löwdin, NAO; S88–S93, S98–S99) and real-space (Becke, Hirshfeld, TFVC; S94–S97, S100–103) atomic definitions, orbital localization (IBOs, Figs. S80–S85), and state-of-the-art effective oxidation state (EOS; Fig. S86; Tables S11–S12) analysis.⁴² Although the results by the various methods are not perfectly consistent, they overall corroborate high covalency as is also found in nickel complexes **i**. and **ii**. Some metrics, such as Mayer's bond order (Mulliken's atomic definition; **2**, $BO \approx 0.9$; **3, 4**, $BO \approx 1.1$; **i**, $BO \approx 1.4$; **ii**, $BO \approx 1.7$) suggest higher nitrene-character for the palladium- than the nickel imido complexes. Also, weak multiple bonding is substantiated by the computed low rotational barriers of the imido ligands (**2** with truncated Dip groups at the ligand: $\Delta E = 15$ kJ mol⁻¹; **3** and **4**: $\Delta E = 3$ kJ mol⁻¹; Figs. S156–S158). Eventually, we used the STEOM-CCSD transition densities (Figs. S77–79) and the CASSCF/NEVPT2 (Fig. S106–S152) calculations to assign the bands in the electronic absorption spectra. The broad bands in the NIR relate to the HOMO–LUMO transition (intra-ligand charge transfer, ILCT), which may be understood alternatively as $p(x)$ to $p(y)$ transition within a nitrene (*cf.* Fig. 4). Conversely, the strong bands in the visible relate to transitions to the S2 and S3 excited states *via* ligand-to-ligand charge transfer (LLCT) from the nitrene- and metal-to-ligand charge transfer (MLCT) to the nitrene ligand. This corroborates the low-valent character of the metal center.

In conclusion, we communicate one crystalline- and the spectroscopic capture of two transient palladium terminal imido complexes. These complexes activate C–H and C–F bonds through nitrene transfer and/or dehydrogenation, and show unusual β -elimination reactivity. Computations, their spectroscopic (UV-Vis, NIR, IR) signatures, and distinguished ambiphilicity suggest substantial palladium(0) character. Current efforts are directed at catalysis and further spectroscopy.

ASSOCIATED CONTENT

Supporting Information. Synthetic procedures, spectroscopic data, computational and crystallographic details. This material is available free of charge via the Internet at <http://pubs.acs.org>.”

AUTHOR INFORMATION

Corresponding Author

* dominik.munz@uni-saarland.de

Funding Sources

We acknowledge financial support by the Fonds der Chemischen Industrie im Verband der Chemischen Industrie e.V. (Liebig Fellowship; D.M.), the German-American Fulbright Commission (Fulbright-Cotrell Award for D.M.) and the Bavarian Equal Opportunities Sponsorship—Realization of Equal Opportunities for Women in Research and Teaching (A.G.). M.G. thanks the Generalitat de Catalunya and Fons Social Europeu for a fellowship (Grant 2018 FI_B 01120). Computational resources by the RRZ Erlangen are gratefully acknowledged. Instrumentation and technical assistance for the XRD analysis of **5** were provided by the Service Center X-ray Diffraction, with financial support from Saarland University and the German Science Foundation DFG (project number INST 256/349-1). EPR spectroscopy was performed using equipment purchased with support of Saarland University and the DFG (project number INST 256/535-1).

ACKNOWLEDGMENT

Support by Karsten Meyer is gratefully acknowledged.

ABBREVIATIONS

CAAC, cyclic (alkyl)(amino) carbene; DFT, density functional theory; EOS, effective oxidation state; EPR, electron paramagnetic resonance; HRMS, high-resolution mass spectrometry; IR, infrared; ILCT, intra-ligand charge transfer; LLCT, ligand-to-ligand charge transfer; MLCT, metal-to-ligand charge transfer; NMR, nuclear magnetic resonance; SC-XRD, single-crystal X-Ray diffraction; Dip, 2,6-diisopropylphenyl.

REFERENCES

- (1) Winkler, J. R.; Gray, H. B., Electronic Structures of Oxo-Metal Ions. In *Electronic Structures of Transition Metal Complexes I*, Springer: Berlin, Heidelberg, 2012; Vol. 142, pp 17-28.
- (2) Mayer, J. M., Why Are There No Terminal Oxo Complexes of the Late Transition Metals? Or the Importance of Metal-Ligand Π Antibonding Interactions. *Comments Inorg. Chem.* **1988**, *8* (4), 125-135.
- (3) Mindiola, D. J.; Hillhouse, G. L., Terminal Amido and Imido Complexes of Three-Coordinate Nickel. *J. Am. Chem. Soc.* **2001**, *123* (19), 4623-4624.
- (4) Waterman, R.; Hillhouse, G. L., Group Transfer from Nickel Imido, Phosphinidene, and Carbene Complexes to Ethylene with Formation of Aziridine, Phosphirane, and Cyclopropane Products. *J. Am. Chem. Soc.* **2003**, *125* (44), 13350-13351.
- (5) Harrold, N. D.; Hillhouse, G. L., Strongly Bent Nickel Imides Supported by a Chelating Bis(*N*-Heterocyclic Carbene) Ligand. *Chem. Sci.* **2013**, *4* (10), 4011-4015.
- (6) Mindiola, D. J.; Waterman, R.; Iluc, V. M.; Cundari, T. R.; Hillhouse, G. L., Carbon-Hydrogen Bond Activation, C-N Bond Coupling, and Cycloaddition Reactivity of a Three-Coordinate Nickel Complex Featuring a Terminal Imido Ligand. *Inorg. Chem.* **2014**, *53* (24), 13227-13238.
- (7) Wiese, S.; McAfee, J. L.; Pahls, D. R.; McMullin, C. L.; Cundari, T. R.; Warren, T. H., C-H Functionalization Reactivity of a Nickel-Imide. *J. Am. Chem. Soc.* **2012**, *134* (24), 10114-10121.
- (8) Dong, Y.; Clarke, R. M.; Porter, G. J.; Betley, T. A., Efficient C-H Amination Catalysis Using Nickel-Dipyrrin Complexes. *J. Am. Chem. Soc.* **2020**, *142* (25), 10996-11005.
- (9) Dong, Y.; Lukens, J. T.; Clarke, R. M.; Zheng, S. L.; Lancaster, K. M.; Betley, T. A., Synthesis, Characterization and C-H Amination Reactivity of Nickel Iminyl Complexes. *Chem. Sci.* **2020**, *11* (5), 1260-1268.
- (10) Dong, Y.; Lund, C. J.; Porter, G. J.; Clarke, R. M.; Zheng, S. L.; Cundari, T. R.; Betley, T. A., Enantioselective C-H Amination Catalyzed by Nickel Iminyl Complexes Supported by Anionic Bisoxazoline (Box) Ligands. *J. Am. Chem. Soc.* **2021**, *143* (2), 817-829.
- (11) Laskowski, C. A.; Miller, A. J.; Hillhouse, G. L.; Cundari, T. R., A Two-Coordinate Nickel Imido Complex That Effects C-H Amination. *J. Am. Chem. Soc.* **2011**, *133* (4), 771-773.
- (12) Carsch, K. M.; DiMucci, I. M.; Iovan, D. A.; Li, A.; Zheng, S. L.; Titus, C. J.; Lee, S. J.; Irwin, K. D.; Nordlund, D.; Lancaster, K. M.; Betley, T. A., Synthesis of a Copper-Supported Triplet Nitrene Complex Pertinent to Copper-Catalyzed Amination. *Science* **2019**, *365* (6458), 1138-1143.
- (13) Grünwald, A.; Suseelan Sarala, A.; Munz, D., Terminal Imido Complexes of the Groups 9–11: Electronic Structure and Developments in the Last Decade. *Eur. J. Inorg. Chem.* **2021**, *2021* (40), 4147-4166.
- (14) Ray, K.; Heims, F.; Pfaff, F. F., Terminal Oxo and Imido Transition-Metal Complexes of Groups 9–11. *Eur. J. Inorg. Chem.* **2013**, *2013* (22-23), 3784-3807.
- (15) Berry, J. F., Terminal Nitrido and Imido Complexes of the Late Transition Metals. *Comments Inorg. Chem.* **2009**, *30* (1-2), 28-66.
- (16) Sun, J.; Abbenseth, J.; Verplancke, H.; Diefenbach, M.; de Bruin, B.; Hunger, D.; Wurtele, C.; van Slageren, J.; Holthausen, M. C.; Schneider, S., A Platinum(II) Metallonitrene with a Triplet Ground State. *Nat. Chem.* **2020**, *12* (11), 1054-1059.
- (17) Schmidt-Räntsch, T.; Verplancke, H.; Lienert, J. N.; Demeshko, S.; Otte, M.; Van Trieste, G. P., 3rd; Reid, K. A.; Reibenspies, J. H.; Powers, D. C.; Holthausen, M. C.; Schneider, S., Nitrogen Atom Transfer Catalysis by Metallonitrene C-H Insertion: Photocatalytic Amidation of Aldehydes. *Angew. Chem. Int. Ed.* **2022**, *61* (9), e202115626.
- (18) Munz, D.; Meyer, K., Charge Frustration in Ligand Design and Functional Group Transfer. *Nat. Rev. Chem.* **2021**, *5* (6), 422-439.
- (19) Wentrup, C., Carbenes and Nitrenes: Recent Developments in Fundamental Chemistry. *Angew. Chem. Int. Ed.* **2018**, *57* (36), 11508-11521.
- (20) Maestre, L.; Sameera, W. M.; Diaz-Requejo, M. M.; Maseras, F.; Perez, P. J., A General Mechanism for the Copper- and Silver-Catalyzed Olefin Aziridination Reactions: Concomitant Involvement of the Singlet and Triplet Pathways. *J. Am. Chem. Soc.* **2013**, *135* (4), 1338-1348.
- (21) Ju, M.; Schomaker, J. M., Nitrene Transfer Catalysts for Enantioselective C-N Bond Formation. *Nat. Rev. Chem.* **2021**, *5* (8), 580-594.
- (22) Olivos Suarez, A. I.; Lyaskovskyy, V.; Reek, J. N.; van der Vlugt, J. I.; de Bruin, B., Complexes with Nitrogen-Centered Radical Ligands: Classification, Spectroscopic Features, Reactivity, and Catalytic Applications. *Angew. Chem. Int. Ed.* **2013**, *52* (48), 12510-12529.
- (23) Grünwald, A.; Munz, D., How to Tame a Palladium Terminal Imido. *J. Organomet. Chem.* **2018**, *864*, 26-36.
- (24) Munz, D., How to Tame a Palladium Terminal Oxo. *Chem. Sci.* **2018**, *9* (5), 1155-1167.
- (25) Broere, D. L.; de Bruin, B.; Reek, J. N.; Lutz, M.; Dechert, S.; van der Vlugt, J. I., Intramolecular Redox-Active Ligand-to-Substrate Single-Electron Transfer: Radical Reactivity with a Palladium(II) Complex. *J. Am. Chem. Soc.* **2014**, *136* (33), 11574-11577.

- (26) Grünwald, A.; Orth, N.; Scheurer, A.; Heinemann, F. W.; Pöthig, A.; Munz, D., An Isolable Terminal Imido Complex of Palladium and Catalytic Implications. *Angew. Chem. Int. Ed.* **2018**, *57* (49), 16228-16232.
- (27) For a palladium-alkylidene, see: Comanescu, C. C.; Iluc, V. M., Synthesis and Reactivity of a Nucleophilic Palladium (II) Carbene. *Organometallics* **2014**, *33* (21), 6059-6064.
- (28) Melaimi, M.; Jazzar, R.; Soleilhavoup, M.; Bertrand, G., Cyclic (Alkyl)(Amino)Carbenes (CAACs): Recent Developments. *Angew. Chem. Int. Ed.* **2017**, *56* (34), 10046-10068.
- (29) Lavallo, V.; Canac, Y.; Präsang, C.; Donnadiu, B.; Bertrand, G., Stable Cyclic (Alkyl)(Amino)Carbenes as Rigid or Flexible, Bulky, Electron-Rich Ligands for Transition-Metal Catalysts: A Quaternary Carbon Atom Makes the Difference. *Angew. Chem. Int. Ed.* **2005**, *44* (35), 5705-5709.
- (30) Chu, J.; Munz, D.; Jazzar, R.; Melaimi, M.; Bertrand, G., Synthesis of Hemilabile Cyclic (Alkyl)(Amino)Carbenes (CAACs) and Applications in Organometallic Chemistry. *J. Am. Chem. Soc.* **2016**, *138* (25), 7884-7887.
- (31) Grünwald, A.; Heinemann, F. W.; Munz, D., Oxidative Addition of Water, Alcohols, and Amines in Palladium Catalysis. *Angew. Chem. Int. Ed.* **2020**, *59* (47), 21088-21095.
- (32) Liu, J.; Bollmeyer, M. M.; Kim, Y.; Xiao, D.; MacMillan, S. N.; Chen, Q.; Leng, X.; Kim, S. H.; Zhao, L.; Lancaster, K. M.; Deng, L., An Isolable Mononuclear Palladium(I) Amido Complex. *J. Am. Chem. Soc.* **2021**, *143* (28), 10751-10759.
- (33) Tentatively, an NH-bridged palladium-dimer forms concomitantly. For further details, see Fig. S58.
- (34) Related reactivity has been reported for iridium: Kinauer, M.; Diefenbach, M.; Bamberger, H.; Demeshko, S.; Reijerse, E. J.; Volkmann, C.; Wurtele, C.; van Slageren, J.; de Bruin, B.; Holthausen, M. C.; Schneider, S., An Iridium(III/IV/V) Redox Series Featuring a Terminal Imido Complex with Triplet Ground State. *Chem. Sci.* **2018**, *9* (18), 4325-4332.
- (35) Kundu, S.; Miceli, E.; Farquhar, E.; Pfaff, F. F.; Kuhlmann, U.; Hildebrandt, P.; Braun, B.; Greco, C.; Ray, K., Lewis Acid Trapping of an Elusive Copper-Tosyl nitrene Intermediate Using Scandium Triflate. *J. Am. Chem. Soc.* **2012**, *134* (36), 14710-14713.
- (36) Moegling, J.; Hoffmann, A.; Thomas, F.; Orth, N.; Liebhäuser, P.; Herber, U.; Rampmaier, R.; Stanek, J.; Fink, G.; Ivanović-Burmazović, I.; Herres-Pawlis, S., Designed to React: Terminal Copper Nitrenes and Their Application in Catalytic C-H Aminations. *Angew. Chem. Int. Ed.* **2018**, *57* (29), 9154-9159.
- (37) Corona, T.; Ribas, L.; Rovira, M.; Farquhar, E. R.; Ribas, X.; Ray, K.; Company, A., Characterization and Reactivity Studies of a Terminal Copper-Nitrene Species. *Angew. Chem. Int. Ed.* **2016**, *55* (45), 14005-14008.
- (38) Gritsan, N. P.; Zhu, Z. D.; Hadad, C. M.; Platz, M. S., Laser Flash Photolysis and Computational Study of Singlet Phenyl nitrene. *J. Am. Chem. Soc.* **1999**, *121* (6), 1202-1207.
- (39) Neese, F., Software Update: The ORCA Program System, Version 4.0. *WIREs Comput. Mol. Sci.* **2018**, *8* (1), e1327.
- (40) For a discussion of the choice of the active space and the position of the coordinate system, see Figs. S106-152; Table S13.
- (41) Thom, A. J.; Sundstrom, E. J.; Head-Gordon, M., LOBA: A Localized Orbital Bonding Analysis to Calculate Oxidation States, with Application to a Model Water Oxidation Catalyst. *Phys. Chem. Chem. Phys.* **2009**, *11* (47), 11297-11304.
- (42) Ramos-Cordoba, E.; Postils, V.; Salvador, P., Oxidation States from Wave Function Analysis. *J. Chem. Theory Comput.* **2015**, *11* (4), 1501-1508.

